Stable knots in the phase diagram of semiflexible polymers: A topological order parameter?

2016 J. Phys.: Conf. Ser. 750 012006

(http://iopscience.iop.org/1742-6596/750/1/012006)

Journal of Physics: Conference Series **750** (2016) 012006 doi:10.1088/1742-6596/750/1/012006

Stable knots in the phase diagram of semiflexible polymers: A topological order parameter?

Wolfhard Janke and Martin Marenz

Institut für Theoretische Physik, Universität Leipzig, Postfach 100 920, 04009 Leipzig, Germany

E-mail: wolfhard.janke@itp.uni-leipzig.de, martin.marenz@itp.uni-leipzig.de

Abstract. We report a recent computer simulation study of the phase diagram of a single semiflexible polymer chain using a generic coarse-grained bead-stick model. The results are obtained with a combination of multicanonical and replica-exchange simulations. Interestingly, we find in the temperature-stiffness plane well-defined phases that can be characterized by stable knots of various types. We discuss how the knots can be observed and to what extent they can be interpreted as "topological order parameter". Another surprising observation concerns the peculiar transitions into these stable knot phases which will be also explained.

1. Introduction

The statistical physics of polymer systems is a very rich field with countless applications ranging from nanotechnology over molecular biology to all kinds of plastics. By stochastically sampling the state space, Monte Carlo (MC) computer simulations provide thermodynamic and structural information of the system. The latter is particularly important for polymers whose typically linear structure gives rise to many different structural motifs [1]. A good example is the phase diagram of a single semiflexible polymer as a function of temperature and bending stiffness [2, 3]. Using a coarse-grained bead-stick continuum model we recently scanned the full range from flexible to stiff polymers and determined the transition lines between phases characterized by well-known structural motifs such as rod-like, collapsed, frozen, bent, and hairpin structures. Among them we also discovered peculiar phases governed by stable knots of various types [3]. Here we give an overview of this study, explain how knots can be detected and why they may be interpreted as "topological order parameter". Finally we also discuss the rather intriguing properties of the transitions into these stable knot phases.

2. Model and simulation methods

In Ref. [3] we considered a minimalistic coarse-grained bead-stick model of a linear semiflexible polymer consisting of N monomers connected by fixed bonds of length r_b. Two terms contribute to the energy [4]:

$$E = E_{\mathrm{LJ}} + \kappa E_{\mathrm{Bend}} = 4\epsilon \sum_{i=1}^{N-2} \sum_{j=i+2}^{N} \left[\left(\frac{\sigma}{r_{ij}} \right)^{12} - \left(\frac{\sigma}{r_{ij}} \right)^{6} \right] + \kappa \sum_{i=1}^{N-2} (1 - \cos\vartheta_i) \ . \qquad (1)$$

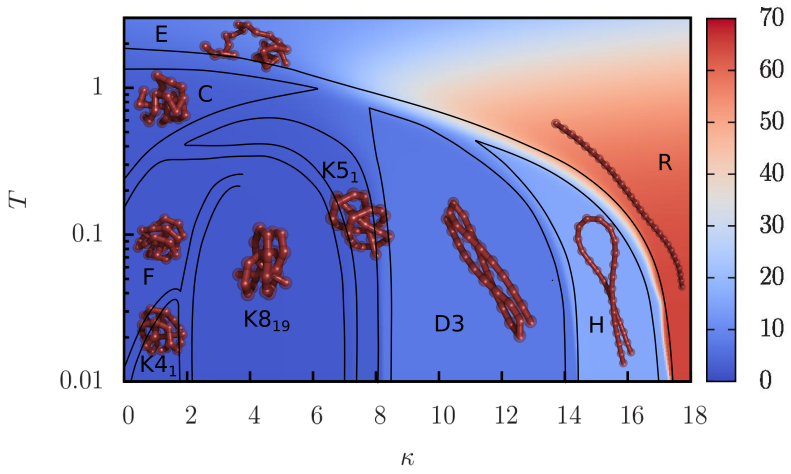

Figure 1. Phase diagram of a semiflexible 28mer in the temperature (T) – bending stiffness (κ) plane (E: elongated, R: rod-like, C: collapsed, F: frozen, K: knotted, DN: $(N-1)$ times bent, H: hairpin). The background color encodes $\langle R^2_{\rm gyr}\rangle$. Note that the temperature is given on a logarithmic scale (taken from Ref. [3]).

The first term is the standard 12–6 Lennard-Jones (LJ) potential, where r_{ij} measures the distance between the monomers i and j. The parameters ϵ and σ set the energy and length scales, respectively, and hence are taken to be $\epsilon = 1$ and $\sigma = 1$ in the following. Note that the minimum of the individual contributions to the LJ potential occurs at $r_{\rm LJ} = 2^{1/6} \approx 1.12 > r_b = 1$. The second term models the bending energy of the polymer similar to a worm-like chain, where $0 \le \vartheta_i \le \pi$ is the angle between adjacent bonds and the parameter κ controls the stiffness strength. For $\kappa = 0$ the polymer is flexible and for large κ it approaches the rod-like limit.

In order to map out the phase diagram in the $T-\kappa$ plane we performed two types of MC studies in generalized ensembles. In the first, we employ a combination of multicanonical simulations with replica exchange in κ direction, and the second is based on a two-dimensional variant of replica exchange in T and κ. In multicanonical ("muca") simulations [5, 6, 7] one replaces the usual Boltzmann weight e^{-E/k_BT} in the canonical partition function by an *a priori* unknown weight function $W(E)$ for polymer configurations x with energy $E(x)$. This results in $Z_{\rm muca} = \sum_x W\left(E\left(x\right)\right) = \sum_E \Omega(E) W(E)$, where $\Omega(E)$ is the density of states. One usually aims at adjusting $W(E)$ such that the multicanonical energy histogram $H(E) \propto P_{\rm muca}(E) = \Omega(E)W(E)$ becomes approximately flat. This can be achieved by starting with $W^{(0)}(E) \equiv 1$ and iterating $W^{(n+1)}(E) = W^{(n)}(E)/H^{(n)}(E)$, where $H^{(n)}(E)$ is the simulated histogram using the weight $W^{(n)}(E)$. The basic idea of replica exchange (or parallel tempering) [8] is to simulate m replicas at different temperatures $k_BT_\mu = 1/\beta_\mu$, $\mu = 1, \ldots, m$, and to propose every now and then an exchange of the configurations x of two replicas μ and ν. To ensure detailed balance, these exchanges are accepted with probability $p\left(x_\mu \leftrightarrow x_\nu\right) = \min\left\{1, \exp\left(\Delta\beta\Delta E\right)\right\}$, where $\Delta\beta = \beta_\mu - \beta_\nu$ and $\Delta E = E(x_\mu) - E(x_\nu)$ are the differences in the inverse temperatures and energies of the two replicas. For a more comprehensive discussion of state-of-the-art simulation and analysis methods in polymer physics, see the recent review [1].

3. Results

The resulting pseudophase diagram for a semiflexible 28mer as obtained in Ref. [3] is shown in Fig. 1. The transition lines were determined by measurements of the two subenergies $\langle E_{\rm LJ}\rangle$

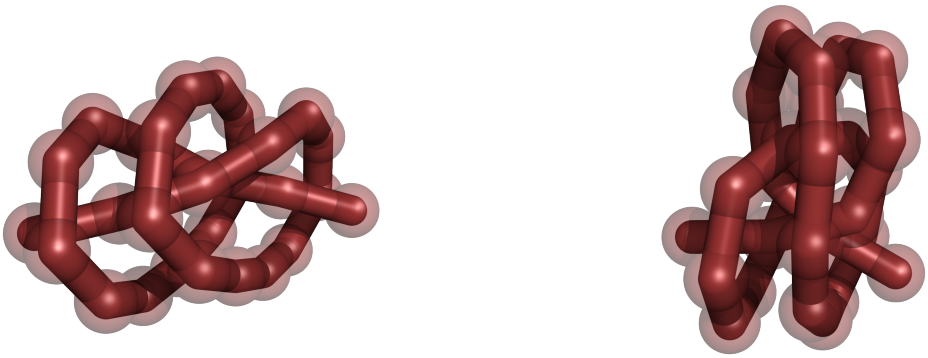

5_1 8_{19}

Figure 2. Typical knots of types 5_1 (at $\kappa = 7.50$, $T = 0.045$) and 8_{19} (at $\kappa = 6.10$, $T = 0.035$) obtained for a semiflexible 28mer.

and $\langle E_{\mathrm{Bend}} \rangle$, the squared end-to-end distance $\langle R_{ee}^2 \rangle$, the squared radius of gyration $\langle R_{\mathrm{gyr}}^2 \rangle$, and the eigenvalues of the gyration tensor $\langle \lambda_1 \rangle$, $\langle \lambda_2 \rangle$, and $\langle \lambda_3 \rangle$. Peaks of the temperature derivative of these observables for a given bending stiffness κ then mark the transition lines in Fig. 1. Due to the finite length of the polymer, different observables give slightly different transition temperatures, which is reflected by the width between the black lines. The background color encodes the average extension of the polymer in terms of $\langle R_{\mathrm{gyr}}^2 \rangle$. We confirmed the thus obtained phase diagram by a microcanonical analysis [9, 10, 11, 12] where one starts from the density of states $\Omega(E)$, calculates the microcanonical entropy $S(E) = k_B \ln \Omega(E)$ and temperature $\beta_{\mathrm{micro}} = dS(E)/dE$, and finally analyzes the peaks in the derivative of $d\beta_{\mathrm{micro}}/dE$ [13].

For high temperatures, the typical conformations are extended (E) or rod-like (R). With decreasing temperature, depending on the bending stiffness, collapsed (C), frozen (F), bent (D3) and hairpin (H) conformations develop. Interestingly, we also observe phases governed by stable knots (K). Two examples are depicted in Fig. 2. Closer inspection reveals that these knots can be identified as $C_n = 4_1$, 8_{19}, and 5_1 knots, where according to the usual classification scheme C counts the minimal number of crossings of any projection of a knot onto a two-dimensional plane and the subscript n distinguishes topologically different knots with the same C. Note that the 5_1 and 8_{19} knots are so-called torus knots, which are known to be formed preferentially in viral DNA [14]. For the identification of the knot type, we employed a method described in Ref. [15] where a specific product $\Delta_p(t) \equiv |\Delta(t) \times \Delta(1/t)|$ of the Alexander polynomial $\Delta(t)$ is evaluated at $t = -1.1$. For definitions and a detailed description of mathematical knot theory, see the book by Kauffman [16].

Mathematically, the identification of knots in *open* polymers is not well defined, so one first has to apply a (virtual) closure prescription. The easiest one would be to draw a virtual bond connecting the two termini of the polymer, but this direct closure results in spurious knots when the polymer is rather compact. In this work we employed the closure CI sketched in Fig. 3(a), which is inspired by tying a real knot. First one connects the two termini of the polymer by a straight line which is then extended in both directions. The two new virtual endpoints A' and B' are located far away from all monomers. A third virtual point C is created on the perpendicular bisector of the connecting line, again far away from all monomers. Finally the polymer can be closed via straight lines connecting C with A' and B', respectively.

For testing purpose we also implemented the second closure CII sketched in Fig. 3(b). Here one increases the bond length of the first and last bond to two new virtual termini A' and B', which are then connected by a straight line to close the polymer. The closures CI and CII give

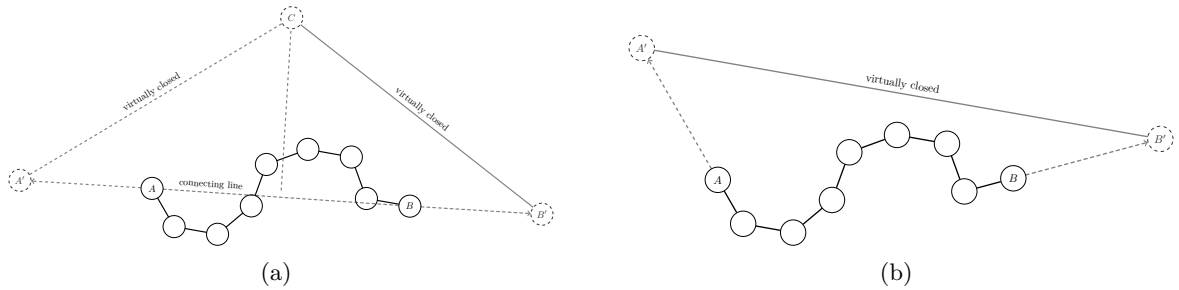

Figure 3. (a) The closure CI moves the termini A and B of the polymer along the line connecting them far outside the polymer to points A' and B', which are then virtually closed by connecting them to a point C on the perpendicular bisector. (b) The closure CII first shifts the two termini A and B to points far outside the polymer and then closes the new virtual termini A' and B'.

qualitatively similar results and are both suitable for identifying the knotted regions. However, with CI all measured conformations are assigned an identical knot type, so $D \equiv \Delta_p(-1.1)$ can be considered as a topological order parameter.

In the study of Ref. [2] using a similar bead-spring model *no* knot phases have been reported. From our own test simulations we suspect that the reason for this difference lies in the choice of the ratio r_{LJ}/r_b, which is 1 in [2] but ≈ 1.12 in our case. If $r_{\mathrm{LJ}}/r_b \approx 1$, then bent conformations are energetically favored over knots. To verify this conjecture, however, more work is necessary.

The transitions from the frozen or bent phases into the knot phases are quite intriguing. As transitions between two structured states, one would expect them to behave first-order-like, similar to other solid-solid transitions. A glance at the inset of Fig. 4 for the D3–$K5_1$ transition suggests, however, that this expectation may not be true since the energy distribution $p(E)$ exhibits only a single peak. There is no indication for the typical double-peak structure at a first-order-like phase transition and hence no signal of latent heat [17, 18]. The true nature of the transition is only revealed when one considers the *two-dimensional* energy distribution $p(E_{\mathrm{LJ}}, E_{\mathrm{Bend}})$, for which indeed two clearly separated peaks are visible in Fig. 4 [3]. The peak in front corresponds to the (unknotted) bent phase D3 and the other in the back to the knot phase $K5_1$. The total energy $E = E_{\mathrm{LJ}} + \kappa E_{\mathrm{Bend}}$ is the projection along the diagonal of this two-dimensional histogram along which the two peaks fall on top of each other, what explains why only a single peak shows up in $p(E)$ and no latent heat is observable.

4. Summary

Using a combination of multicanonical and replica-exchange simulations, we mapped out the phase diagram for a generic bead-stick model of a semiflexible polymer. Besides the structural motifs already observed in previous work, we found transitions into novel phases governed by thermodynamically stable knots of various types, which may be considered as a topological order parameter. Their properties are considerably different from those of knots observed in the swollen and globular phases of flexible polymers, which form by chance. The second intriguing observation is that the transitions into these knotted conformations from other structured states happen with almost no latent heat, although we observed a clear phase coexistence.

Acknowledgments

This work was supported by the European Union and the Free State of Saxony, the Leipzig Graduate School of Natural Sciences "BuildMoNa", the Deutsche Forschungsgemeinschaft through Sonderforschungsbereich/Transregio SFB/TRR 102 (Project B04), and the Deutsch-

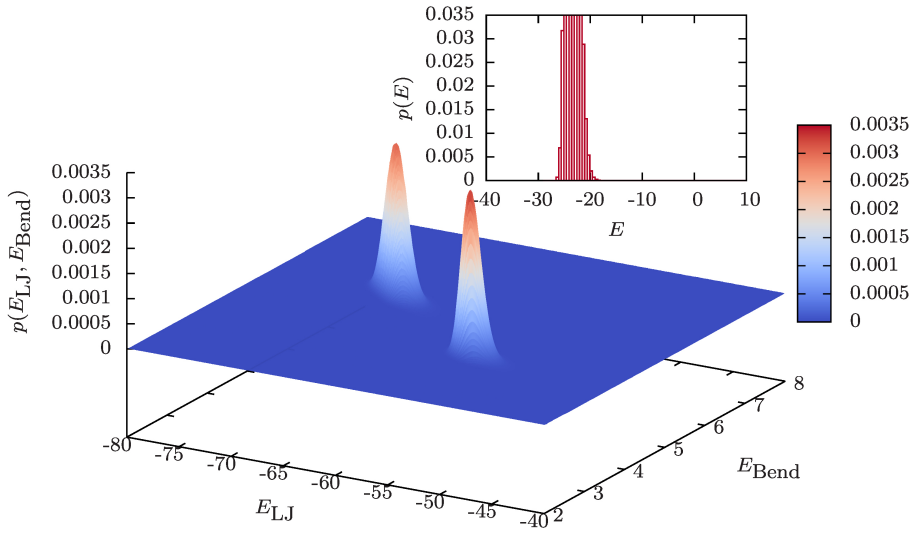

Figure 4. Two-dimensional energy histogram $p(E_{\mathrm{LJ}}, E_{\mathrm{Bend}})$ of a 28mer at the D3–K5$_1$ transition for $\kappa = 8.0$ at $T = 0.18$, signaling clear phase coexistence. The inset shows the one-dimensional energy histogram $p(E)$ of the total energy $E = E_{\mathrm{LJ}} + \kappa E_{\mathrm{Bend}}$, which corresponds to a projection along the diagonal of the two-dimensional histogram. In this projection, the two peaks fall on top of each other, so only a single peak is visible in $p(E)$.

Französische Hochschule (DFH-UFA) through the International (Leipzig-Lorraine-Lviv-Coventry) Doctoral College for the Statistical Physics of Complex Systems "$\mathbb{L}^4$" under Grant No. CDFA-02-07. Special thanks goes to the John von Neumann Institute for Computing (NIC) for granting computing time provided on the supercomputer JUROPA at Jülich Supercomputing Centre (JSC) under Grant No. HLZ21.

References

[1] Janke W and Paul W 2016 *Soft Matter* **12** 642-657
[2] Seaton D T, Schnabel S, Landau D P and Bachmann M 2013 *Phys. Rev. Lett.* **110** 028103-1-5
[3] Marenz M and Janke W 2016 *Phys. Rev. Lett.* **116** 128301-1-6
[4] Bachmann M, Arkın H and Janke W 2005 *Phys. Rev.* E **71** 031906-1-11
[5] Berg B A and Neuhaus T 1991 *Phys. Lett.* B **267** 249-253
[6] Berg B A and Neuhaus T 1992 *Phys. Rev. Lett.* **68** 9-12
[7] Janke W 1992 *Int. J. Mod. Phys.* C **3** 1137-1146
[8] Hukushima K and Nemoto K 1996 *J. Phys. Soc. Jpn.* **65** 1604-1608
[9] Gross D H E 2001 *Microcanonical Thermodynamics* (Singapore: World Scientific)
[10] Janke W 1998 *Nucl. Phys.* B (Proc. Suppl.) **63A-C** 631-633
[11] Junghans C, Bachmann M and Janke W 2006 *Phys. Rev. Lett.* **97** 218103-1-4
[12] Junghans C, Bachmann M and Janke W 2008 *J. Chem. Phys.* **128** 085103-1-9
[13] Schnabel S, Seaton D T, Landau D P and Bachmann M 2011 *Phys. Rev.* E **84** 011127-1-4
[14] Reith D, Cifra P, Stasiak A and Virnau P 2012 *Nucleic Acids Res.* **40** 5129-5137
[15] Virnau P 2010 *Physics Procedia* **6** 117-125
[16] Kauffman L H 1991 *Knots and Physics* 2nd ed. (Singapore: World Scientific)
[17] Janke W 1993 *Phys. Rev.* B **47** 14757-14770
[18] Janke W 2003 in: *Computer Simulations of Surfaces and Interfaces*, NATO Science Series, II. Mathematics, Physics and Chemistry – Vol. **114**, edited by B. Dünweg, D. P. Landau and A. I. Milchev (Dordrecht: Kluwer), pp. 111-135